

<https://doi.org/10.15407/dopovidi2026.02.046>

UDC 621.521; 533.15

**G.P. Glazunov**, <https://orcid.org/0000-0002-8895-927X>

**M.M. Bondarenko**, <https://orcid.org/0000-0001-5783-9788>

**O.L. Konotopskyi**, <https://orcid.org/0000-0002-1622-6376>

National Science Center “Kharkiv Institute of Physics and Technology”  
of the NAS of Ukraine, Institute of Plasma Physics, Kharkiv, Ukraine  
E-mail: glazunov@ipp.kharkov.ua

## Kinetics of hydrogen outgassing and absorption by palladium in molecular driven and electrolysis regimes

Presented by Academician of the NAS of Ukraine I.Ye. Garkusha

*Experimental investigations of the kinetics of hydrogen saturation and outgassing from palladium have been carried out in conditions of interaction with molecular and electrolytic hydrogen at near room temperature and the pressure range of 1–2 at. Using the gravimetric method, it was established that the rate of hydrogen saturation during electrolysis is more than two orders higher than in the molecular driven regime. With help of mass-spectrometric method it has been shown that in the course of hydrogen absorption by Pd cathode during electrolysis and subsequent heating process in high vacuum, the ultra-pure hydrogen (higher than 99.999 vol. %) is generated.*

*Based on the measured temperature dependence of hydrogen evolution, the activation energy of hydrogen outgassing from the Pd-cathode after one-hour exposure to electrolysis ion current  $\approx 8$  A was calculated to be  $E \approx 23$  kJ/mol or  $\approx 12$  kJ/mol, in dependence on the temperature range (20–100 °C or 300–650 °C). The average value of activation energy for the whole temperature range of the performed measurements was estimated as  $\approx 22.4$  kJ/mol. Therefore, hydrogen outgassing from PdHx system could be multi-stage process with ever-changing activation energy on time. The physical-chemical mechanisms and the influence of  $\beta \leftrightarrow \alpha$  transition in the PdHx system are further discussed and analyzed to explain such hydrogen behavior during the outgassing process.*

**Keywords:** hydrogen, palladium, electrolysis, activation energy, absorption, outgassing.

**1. Introduction.** The kinetics of hydrogen behavior on palladium has been thoroughly studied previously [1]. It has been established that hydrogen penetration from gas phase into metal lattice (absorption) occurs through several main stages: (i) dissociation of chemisorbed molecules, (ii) transition of hydrogen atoms through the gas-metal boundary into near surface bulk of metal, (iii) diffusion of hydrogen atoms (ions) into metal bulk. At the hydrogen release from metal lattice, all these stages occur in the reverse order. If the rate of process is limited by dissociation  $\leftrightarrow$  recombina-

---

Citation: Glazunov G.P., Bondarenko M.M., Konotopskyi O.L. Kinetics of hydrogen outgassing and absorption by palladium in molecular driven and electrolysis regimes. *Dopov. nac. akad. nauk Ukr.* 2026. No. 2. P. 46–56. <https://doi.org/10.15407/dopovidi2026.02.046>

© Publisher PH «Akademperiodyka» of the NAS of Ukraine, 2026. This is an open access article under the CC BY-NC-ND license (<https://creativecommons.org/licenses/by-nc-nd/4.0/>)

tion processes, then saturation rate is proportional to hydrogen pressure  $P$  and the outgassing rate is proportional to hydrogen concentration as  $c^2$ . When the second/third stages limit the process rate, absorption became proportional to  $P^{1/2}$ , and outgassing rate proportional to concentration  $c$ . It should be noted that the rate of absorption-desorption processes strongly depends on the state of metal surface (mainly on the poison impurities presence, especially carbon and their concentration), temperature, pressure, rates of surface reactions of dissociation↔recombination, sample dimensions, diffusion coefficient, state of hydrogen (molecules or atoms and ions), etc. In the Pd bulk the latter can drive changes from  $\alpha$  to  $\beta$  phase (from solution to metal hydride state).

In previous works [2—4], the dynamics of hydrogen interaction with Pd-cathodes under electrolysis conditions were investigated in comparison with hydrogen in the molecular state. In particular, it was shown that hydrogen saturation rate of Pd during electrolysis process essentially higher than that in molecular hydrogen driven regime. It was also noted that only a part of hydrogen ( $\approx 14\%$  in [2] and  $\approx 40\%$  in [4]), produced during electrolysis, can be used for cathode saturation and ultra-pure hydrogen production. The main quantity of produced electrolytic hydrogen (explosive gas, Brown's gas) can be used in others technological processes, e.g., for fuel or explosive production. It may provide low prime cost of produced ultra-pure hydrogen, which is widely used in chemical and electronic industries, gas chromatography, fuel cells, as well as in different researches, which carried out in many laboratories, etc.

This work has been performed with the aim to examine in greater detail the kinetics of palladium saturation with hydrogen molecular and electrolytic gas. Particular attention was paid to the possible influence of  $\alpha \leftrightarrow \beta$  transition in Pd [1, 5] on the Pd-cathode characteristics, such as hydrogen sorption and outgassing rate. This is important, in particular, for optimization technology processes of ultra-pure hydrogen production during electrolysis, achievement of maximum hydrogen capacity of Pd-cathodes, increasing their life time and overall efficiency, substantial reduction of saturation time and produced gas depreciation.

## **2. Experimental setup and methods.**

**2.1. Experimental setup and equipment.** A schematic view of the GAS (Gassing and Sorption) experimental installation is shown in Fig. 1. This experimental stand has been designed to measure mass-spectra and characterize degassing and sorption processes. It includes a vacuum chamber 1 made of stainless steel 12Cr18Ni10Ti. Chamber 1 is connected via valves 3 and 7 to a pumping and gases inflow systems. Pumping system consists of cryogenic pump 4, M-500 diffusion pump 5, and 3NVR-1D fore vacuum pumps 6.

The vacuum system is equipped with PMT-4M thermocouple gauges 9, PMI-10 (10), PMI-2 ionization gauges 11, and MX-7304 (Sumy, Ukraine) mass spectrometer 8. Instrument readings recorded using the WAD-AIK-BUS analog module (Kyiv, Ukraine) and a computer. Before experiments, the chamber and sample were heated to  $\approx 100\text{ }^\circ\text{C}$  during one hour, that allows achievement of ultrahigh vacuum  $1\text{--}5 \cdot 10^{-7}$  Torr to carry out sorption, thermal degassing, and mass spectrometric measurements with sufficient accuracy.

Gases puffing system includes an electrolyzer 17, E-4 model (Fig. 2), hydrogen saturation chamber 18, and balloons 14, 15, 16 with pure (99.99 vol. % purity) Ar,  $\text{H}_2$ , and He. The high-pressure valves 12, 13, fine inlet valve 7 and pressure gauge 19 provide inputting and pressure measuring of any type of gases.

Samples for our studies were the 99.98 wt. % pure palladium tubes, which served as cathodes in the electrolyzer 17, and five Pd-disks (numbers N1—N5) of 25 mm diameter and 0.3 mm thick-

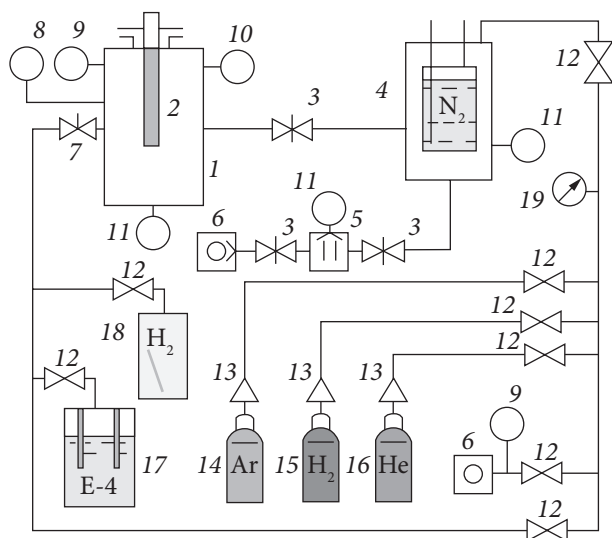


**Fig. 1.** The scheme of experimental setup: 1 — GAS vacuum chamber; 2 — sample; 3 — gate valves; 4 — cryogenic pump; 5 — diffusion pump M-500; 6 — fore vacuum pumps 3NVR-1D; 7 — inlet valve; 8 — mass spectrometer MX-7304; 9 — thermocouple gauges PMT-2; 10 — ionization gauge PMI-10; 11 — ionization gauge PMI-2; 12 — high pressure valves; 13 — gas reducers; 14, 15, 16 — argon, hydrogen, helium balloons; 17 — E-4 model electrolyzer; 18 — chamber for hydrogen saturation of samples; 19 — pressure gauge

ness. The similar Pd-disks N6 and N7, but with 1mm thickness and coated by W films of 2  $\mu\text{m}$  and 4  $\mu\text{m}$  thickness manufactured by vacuum plasma deposition method [6–9] were tested too.

A schematic view of the electrolyzer 17 (E-4) is shown in Fig. 2. It consists of chamber 1 made of stainless steel 12Cr18Ni10Ti and filled with electrolyte. In chamber 1, three Pd-cathodes 3 in form of tubes with diameter of  $3 \times 1$  mm and length of 200 mm, are placed. One end of the tubes was hermetically sealed by brazed with silver welding alloy. Cathodes 3 are electrically connected to flange 5 through flange fittings. The chamber 1 through fluoroplastic isolator 4 was mechanically connected to the flange 5. The body of chamber 1 served as anode.

Chamber 1 (see Fig. 2) provides the technical ability to place various samples for studying cathode hydrogen saturation. To measure the electrolyte temperature a thermocouple could be installed through fluoroplastic seal-insulators 6. The pressure value in the electrolysis chamber 1 is measured by pressure manometer 9. Water seal 7 ensures the safe venting of excess hydrogen into the atmosphere.

Part of the electric potential could be applied to the anode and cathodes from a power supply consisting of a rectifier on two V200 diodes, connected through current transformer to autotransformer. The solution  $\text{H}_2\text{O} + 1$  wt. %  $\text{NaHCO}_3$  or  $\text{Na}_2\text{CO}_3$  (soda ash), was used as an electrolyte. Hydrogen is produced by electrolysis in the chamber 1 similar as in works [3, 4]. In Fig. 3 the current-voltage characteristics of the electrolysis process are shown. It is seen that number of cathodes, either one or three, has no essential influence on electrical characteristics.

Hydrogen saturation chamber 18 (see Fig. 1) provided the technical ability to saturate various Pd samples in hydrogen atmosphere at different pressures. Before being placed in the chamber, the samples were cleaned with following procedures: wiping with special fabric wetted in clean branded gasoline (benzene), drying, wiping with special fabric wetted in 96–99 vol. % ethanol, drying. Similar procedure was used before placing the samples in the vacuum chamber of GAS. Each sample was weighted on the VLR-200 balance and placed in the chamber. Chamber volume was pumped to the pressure of  $\approx 10^{-4}$ – $10^{-3}$  Torr. After that, hydrogen from the balloon 15 (see Fig. 1) inlet to chamber for the required pressure. The samples were exposed to hydrogen during 0.5–312 hours, then, were demounted and weighted, to determine absorbed hydrogen quantity.

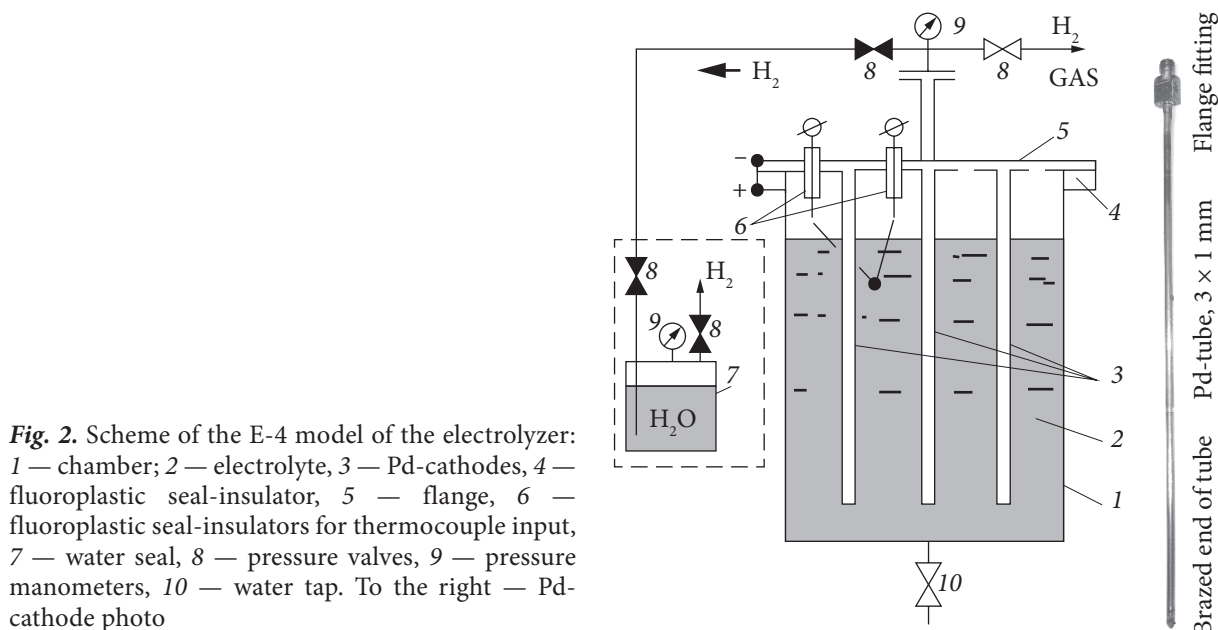


**Fig. 2.** Scheme of the E-4 model of the electrolyzer: 1 — chamber; 2 — electrolyte, 3 — Pd-cathodes, 4 — fluoroplastic seal-insulator, 5 — flange, 6 — fluoroplastic seal-insulators for thermocouple input, 7 — water seal, 8 — pressure valves, 9 — pressure manometers, 10 — water tap. To the right — Pd-cathode photo

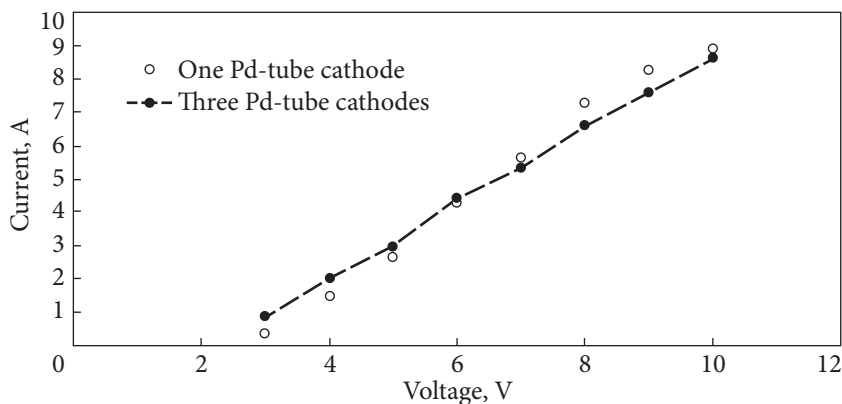


**Fig. 3.** Current-voltage characteristics under electrolysis process in the electrolyzer E-4

**2.2. Experimental methods and results.** During the experiments, the following characteristics have been measured:  $Q$  (Normal  $\text{cm}^3 \text{H}_2$ ,  $\text{Ncm}^3$ ) or  $\nu$  ( $\text{Ncm}^3/\text{g Pd}$ ) — volumetric quantity of hydrogen absorbed by palladium in dependence on the time  $t$  of saturation in the molecular/electrolytic hydrogen,  $\text{PdH}_x$  — number  $x$  of hydrogen atoms per palladium atom;  $S$  ( $\text{Ncm}^3/(\text{g} \cdot \text{h})$ ) — saturation rate;  $q$  ( $\text{Ncm}^3/\text{s}$ ) — hydrogen outgassing rate. Hydrogen quantity  $Q$  was calculated as the difference between the sample mass before and after hydrogen saturation (weighting method). Estimates were also made by integrating the gas quantity, pumped during sample heating in vacuum.

After Pd-sample placing in the high vacuum chamber of the GAS stand and subsequent pumping to the pressure of  $\sim 10^{-7}$  Torr, careful measurements of mass-spectra (Fig. 4), and the dependences of the hydrogen outgassing rate on the temperature were carried out using the methods, similar to those described in [2—4]. The samples (cathodes) were heated by direct current up to temperatures of 20—650 °C and, simultaneously, the pressure time dependence and mass-spectra of desorbed gases was measured (Fig. 4, 5). Apparatus curves were processed to obtain data

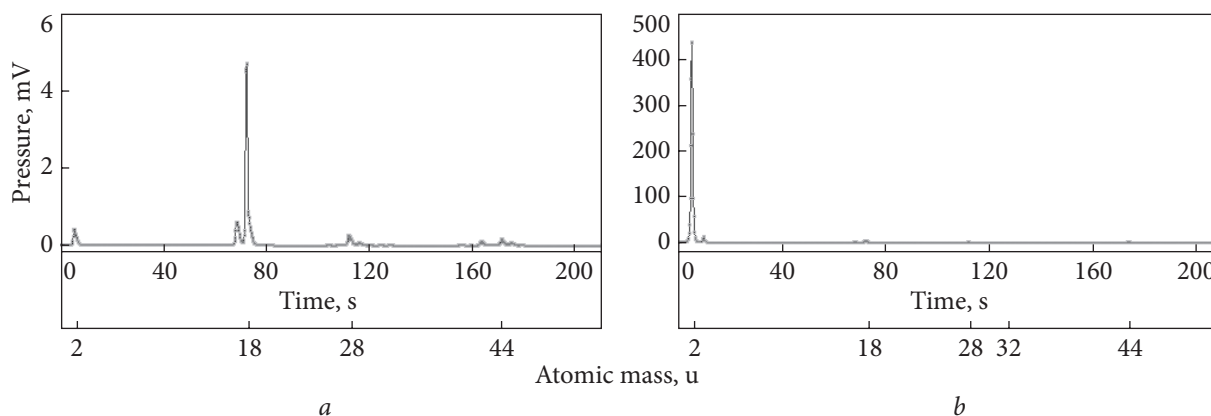


**Fig. 4.** Mass spectra of gases in the GAS chamber before sample heating (a), and (b) during Pd-cathode heating at 120 °C

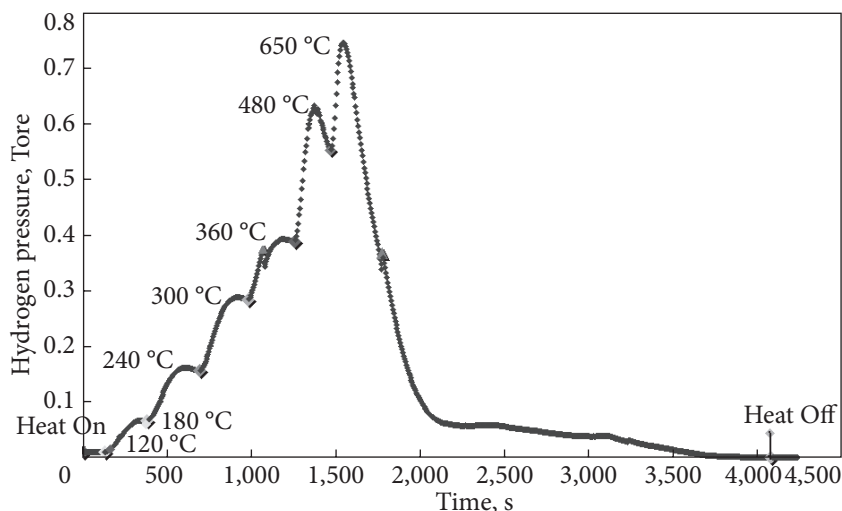


**Fig. 5.** Apparatus curve of pressure change in the vacuum chamber during Pd-cathode heating

for estimating the hydrogen amount desorbed from the sample by the equation:  $Q = (P - P_0)st$ , where  $Q$  is hydrogen quantity, Torr·l or Ncm<sup>3</sup>;  $P$  — maximum pressure, Torr;  $P_0$  — initial pressure, Torr;  $s$  — pumping speed, l/s;  $t$  — time, s. It is necessary to take into account that the sensitivity of the mass spectrometer for hydrogen is approximately two times lower than for air. For the pressure measurement with a gauge PMI-10, this coefficient is four. Also an important factor during the outgassing rate measurements is the change of pumping speed caused by strong pressure increase from  $\sim 10^{-7}$  Torr up to 1 Torr, when diffusion pump did not work ( $s \approx 100$  l/s) and only fore-vacuum pumping ( $\sim 1$  l/s) occurred. Thus, reliable data on the temperature outgassing rate dependence are applied to the ranges of 20–120 °C and 300–650 °C. The analyzed gas was released into vacuum chamber to a pressure of  $10\text{--}0.5 \cdot 10^{-5}$  Torr. Instrument readings were recorded using the WAD-AIK-BUS analog module and PC.

Processing of the instrumental spectra showed that at the electrolyte temperature of  $\approx 50\text{--}60$  °C and the pressure in the electrolyze chamber of 1 at, the generated gas consists of hydrogen

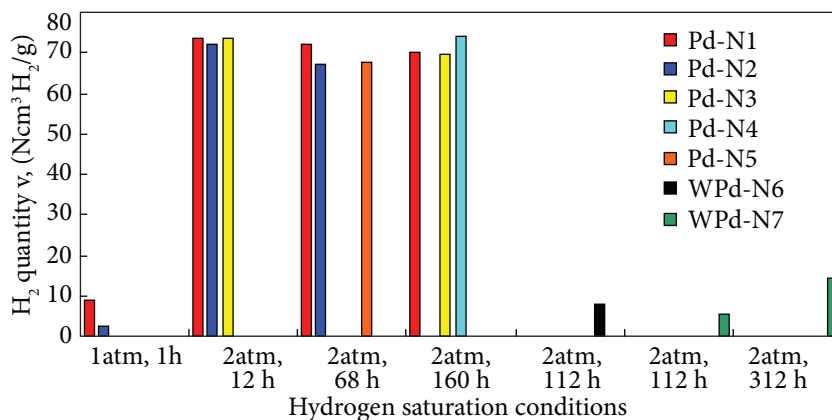


Fig. 6. Hydrogen amount absorbed in Pd foils v/s time of saturation

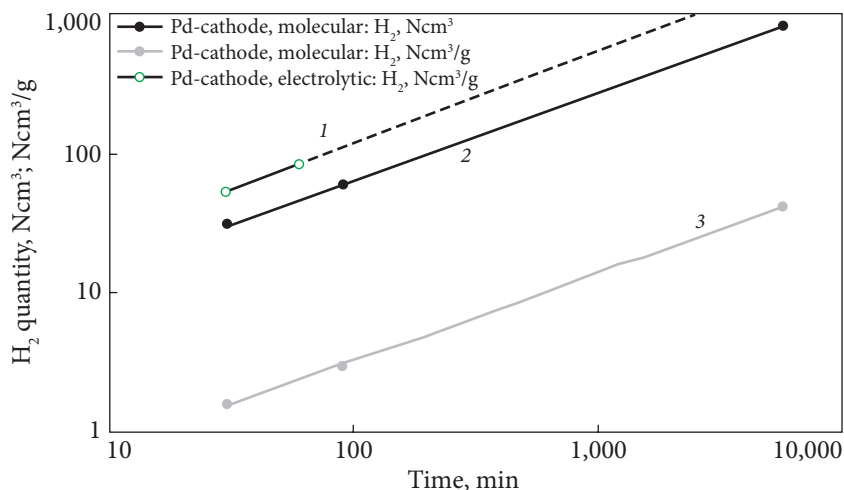
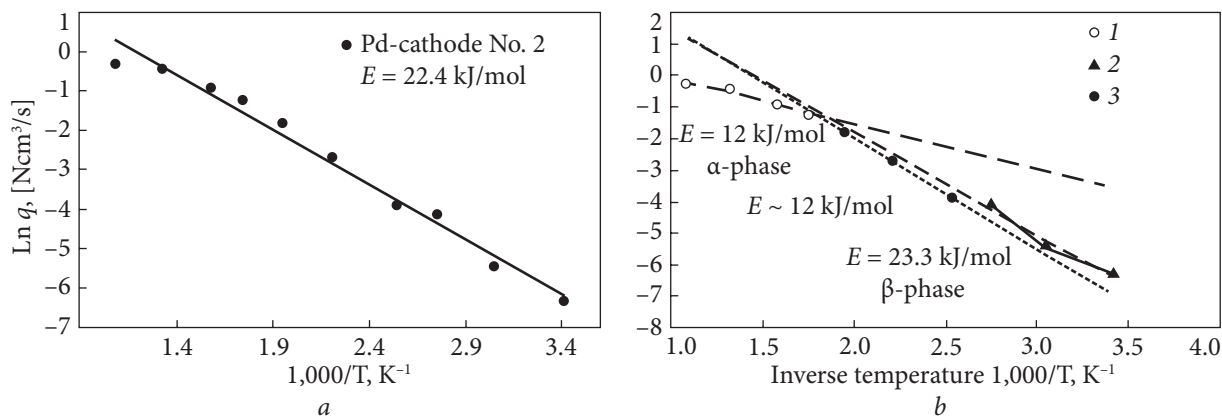


Fig. 7. Hydrogen quantity absorbed in Pd tube-cathode N2 v/s time of saturation in molecular hydrogen (points 2, 3), and in electrolytic regime (points 1)

of 92–94 vol. % purity [4]. The gas desorbed upon heating in a vacuum from Pd-cathode (see Fig. 4, *b*), is found to be ultra-pure (better than 99.999 vol. %) hydrogen. Small marks of the water presence, CO, CO<sub>2</sub> caused by gases desorption from chamber walls. The main impurity was H<sub>2</sub>O ( $\approx 5$  mV mass-spectrometer signal of 18 mass units in Fig. 4, *a*).

Fig. 6 presents hydrogen saturation data for N1–N5 samples (Pd disks with a diameter of 25 mm, a thickness of 0.3 mm) and N6, N7 samples (one-sided W-coated Pd-disks with the same diameter and 1mm thickness) in dependence on the saturation time at pressure of 1–2 atm and at room temperature.

In Fig. 7 the data on hydrogen saturation of annealed in a vacuum Pd-cathode in the case of molecular and electrolytic hydrogen are shown. The results of measurements of the temperature dependence of hydrogen outgassing rate  $q$  for the Pd cathode N2 are presented in Fig. 8. Using these data, the value of activation energy  $E$  of outgassing process could be calculated from the slope of  $\ln(q) = -b - E/RT$  straight lines similarly to described in [6–9]. It was assumed that the



**Fig. 8.** Inverse temperature dependence of hydrogen outgassing rate for the  $\text{PdH}_x$ -cathode N2 (a); b: points 1 — temperature range during sample heating was 300—650°C; points 2 — temperature range was 20—90°C; points 3 — temperature range was 120—240 °C

process of gas evolution obeys Fick's diffusion laws, and the temperature dependence obeys the Arrhenius equation:  $q(T) \sim b \cdot e^{-E/RT}$ . The activation energy for outgassing would be  $E = E_d + E_{des}$ , where  $E_d$  is the activation energy of diffusion and  $E_{des}$  is the activation energy of desorption.

### 3. Discussion.

**3.1. Molecular hydrogen absorption by Pd.** The activation energy of the hydrogen saturation  $E_{sat} = E_{abs} + E_d$  consists of the absorption (solution) activation energy  $E_{abs}$  and the diffusion activation energy  $E_d$ . In our case, for hydrogen flow to/from metal volume one can write the next equation:

$$q = a l^{-1} t^{-1} F^{-1} \Delta c(T, P) e^{-(E_d + E_{abs/des}) / RT},$$

where  $a$  — constant,  $l$  — sample thickness,  $F$  — sample surface area,  $t$  — time,  $\Delta c$  — gradient of concentration. Pressure  $P$  and temperature  $T$  are, in turn, functions of time.

As shown in Fig. 6, within the saturation time range 12—160 hours the hydrogen quantity  $\nu$  in different samples N1—N5 is nearly 70  $\text{Ncm}^3/\text{g}$  ( $Q \approx 90 \text{ Ncm}^3 \text{ H}_2$ ,  $\text{H}/\text{Pd} = 0.6\text{—}0.7$ ). Saturation rate  $S = Q/mt \approx 6$  ( $\text{Ncm}^3/(\text{g}\cdot\text{h})$ ), where  $m$  is sample mass, grams, and  $t$  is saturation time, hours. According to published data [1, 5], a Pd-sample with the mass of 1.3 g could absorb approximately 132  $\text{Ncm}^3 \text{ H}_2$ . This difference may be attributed to different sorption properties of the sample surface and the presence of poison impurities in the saturation chamber. The key point is that as the saturation time increases from 12 to 160 hours, there is a slight decrease (approximately 5%) in the amount of absorbed hydrogen. Incidentally, if the chamber during long time saturation is pumped several times and filled by “fresh” hydrogen from balloon, the  $\nu$  value for sample N4 coincides with the data for sample N1 ( $\approx 74 \text{ Ncm}^3 \text{ H}_2/\text{g}$ ).

Hydrogen saturation process of samples N1—N5 occurs on both their sides. It is known that hydrogen in Pd has a low binding energy ( $\approx 0.23 \text{ eV}$  [10]) and high mobility at moderate and even at low temperatures. At room temperature, the hydrogen diffusion coefficient in  $\alpha$ -phase equals  $3.8 \cdot 10^{-7} \text{ cm}^2/\text{s}$  and in  $\beta$ -phase  $2 \cdot 10^{-7} \text{ cm}^2/\text{s}$  [1, 5]. Therefore, saturation of such samples to maximum hydrogen concentration  $\text{H}/\text{Pd} \approx 0.5\text{—}0.7$  occurs rather quickly (10—12 hours).

For samples N6 and N7 with single-sided W coating, the quantity of absorbed hydrogen is much lower ( $Q = 35$  and  $46 \text{ Ncm}^3$ , accordingly) even if very long time of saturation (112 h). When the satu-

**Fig. 9.** Potential diagram of hydrogen interaction in W-Pd system:  $E_d$  is the activation energy of desorption and recombination,  $E_s$  is the activation energy of solution,  $E_{D_0}$  is the activation energy of hydrogen diffusion in W-film bulk,  $E_{D_s}$  is the activation energy of hydrogen diffusion in the subsurface layer of thickness  $2\lambda$

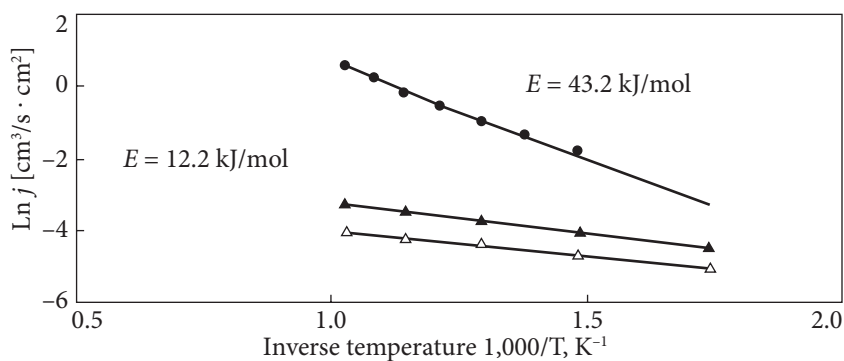
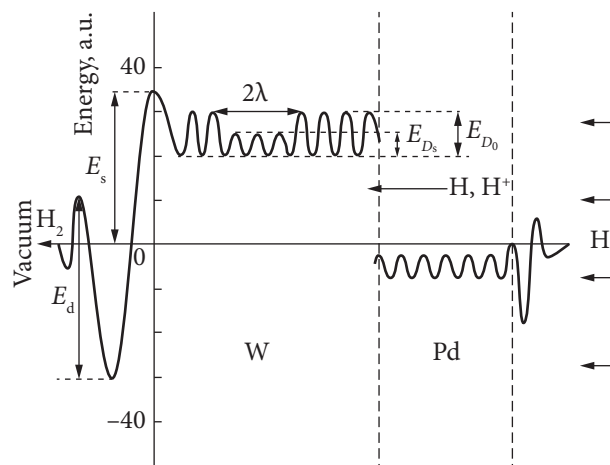


**Fig. 10.** Hydrogen penetration flow  $j$  through bare Pd (dark circles) and through W-Pd two-layer systems (dark triangles —  $2 \mu\text{W}$ ; white triangles —  $4 \mu\text{W}$ ) v/s inverse temperature

ration time was increased to 312 hours (sample N7), the volumetric quantity of absorbed hydrogen grew up to  $\approx 86 \text{ Ncm}^3 \text{ H}_2$  ( $\approx 14 \text{ Ncm}^3 \text{ H}_2/\text{g}$  or  $1.5 \cdot 10^{-4} \text{ Ncm}^3/(\text{g} \cdot \text{h})$ ), i.e., very slow saturation of Pd takes place. It seems that W-Pd interface is the efficient barrier for the hydrogen diffusion flow from the open side of the sample. From the diagram Fig. 9, reproduced from the work [7], it is evident that the activation energy of hydrogen solution  $E_s$  for W indeed is much higher than for Pd.

Hydrogen in W lattice is strongly bound up with host atoms (the bond energy is approximately 1.04 eV [13]). All of this indicates tungsten is one of the most hydrogen resistible materials. Therefore, it is likely that the amount of hydrogen dissolved in the tungsten film from the side facing to molecular gas can be neglected.

The other side (W-Pd system interface) interacts more effectively with hydrogen atoms or ions incoming from Pd-lattice. Moreover, the hydrogen gas in the Pd lattice can be ionized, and the state similar to the plasma [11] or strong non-ideal plasma [12, 13] state might appear. In [7], it was shown that Pd-substrate plays in this case the role of the original “compressor”, which provides significant increase of hydrogen pressure (both H-atoms and ions) in near subsurface interface bulk of W-film (20 and 40 at. instead of 1–2 at.). As it is seen in Fig. 10 [7], penetration through W-Pd interface was the limiting stage of hydrogen permeation in the bimetallic system W-Pd. Activation energy of this process was very low,  $\approx 12$  kJ/mole, which is significantly lower than for

bulky bare tungsten or palladium. Thus, this near interface bulk of W-film quickly saturates up to high concentration and serves as barrier against hydrogen diffusion through Pd-substrate (due to first Fick's law diffusion flow is proportional to concentration gradient [1]). This process could be the reason of very slow hydrogen saturation of W one-side coated Pd in compare with bare Pd.

**3.2. Electrolytic hydrogen absorption by Pd.** The hydrogen saturation process of Pd-tube cathodes was analyzed in detail in our previous work [4]. It was estimated that at an electrolytic current of 8 A, the actual flow of hydrogen ions to the cathode is  $1.1 \cdot 10^{23} \text{ H}^+$ . This corresponds to about 2 liters of electrolytic hydrogen gas at normal conditions. In our case, one Pd-cathode with mass of 14.5 g (volume  $1.25 \text{ cm}^3$ ) absorbs during 1 h electrolysis process in above mentioned regime  $840 \text{ Ncm}^3 \approx 0.8 \text{ liter of H}_2$  ( $58 \text{ Ncm}^3/\text{g}$ ). In other words,  $\approx 40 \%$  of produced electrolytic hydrogen could be converted into ultra-pure hydrogen.

The volumetric amount of hydrogen  $\nu$  ( $\text{Ncm}^3 \text{ H}_2/\text{g}$ ) absorbed by Pd-tube cathode N2 during 1 hour electrolysis (see Fig. 7, 1) is  $\approx 80$ . For molecular driven regime, this value is only  $\approx 50$  after 94 hours exposure at 2 at pressure. This corresponds to the saturation rates 80 and  $0.53 \text{ Ncm}^3/(\text{g} \cdot \text{h})$ , accordingly. Such large difference can be caused by different state of hydrogen (more active atoms and ions instead of molecules) during saturation process in the electrolyzer.

**3.3. Hydrogen outgassing from Pd-cathode.** As can be seen in Fig. 8, a, the experimental data allow conclusion that essential deviation from the Arrhenius law actually observed in the temperature dependence of Pd-cathode outgassing. We think that  $\beta \leftrightarrow \alpha$  transition in Pd might influence on the process which could be composed of several consecutive stages (see Fig. 8, b). At the beginning of Pd sample heating (first stage, temperature range is 20—100 °C), hydrogen in metal bulk remains mainly in  $\beta$ -phase (according to [1] only 0.008—0.03 H/Pd is in  $\alpha$ -phase), diffusion coefficient is rather low and the activation energy calculated to be  $\approx 23 \text{ kJ/mol}$  (see Fig. 8, b, curve 2).

As the temperature rises (100—300 °C), the second stage transition occurs (curve 3 in Fig. 8, b). Hydrogen transitions from hydride state to solution state (from  $\beta$ - to  $\alpha$ -phase), and both phases coexist. Concentration of  $\alpha$ -phase increases up to  $\approx 20 \%$  ( $\text{H/Pd} = 0.21$  [1]). As noted above, the pumping speed in this stage strongly decreased (from 100 to 1 l/s). Unfortunately, we did not have the technical possibility to measure this change precisely; therefore, the data in this temperature range (curve 3 in Fig. 8, b) are not sufficiently reliable. With a further temperature increase (third stage, 300—650 °C), hydrogen concentration in Pd decreases as the result of high outgassing rate, and mainly  $\alpha$ -phase state is realized in Pd sample. Activation energy of outgassing for this temperature region is calculated to be  $E \approx 12 \text{ kJ/mol}$ , i.e., approximately half as much. Note that a similar interpretation to explain hydrogen electro-sorption process by the  $\alpha \leftrightarrow \beta$  transition in the thin Pd-Ni films was given in [14]. If to calculate an average value of activation energy for whole temperature range the measurements carried out in (see Fig. 8, a), it has to be  $E \approx 22.4 \text{ kJ/mol}$ . Thus, hydrogen evolution from  $\text{PdH}_x$  system in this case is complete, multi-stage process with ever-changing activation energy on time.

**Conclusions.** The current-voltage characteristics of the electrolysis process have been measured for the developed E-4 electrolyzer model. It was observed that the change of number of cathodes from one to three has no essential influence on electric characteristics of the electrolyzer.

After hydrogen absorption by Pd cathode during electrolysis, and with subsequent heating it in high vacuum, ultra-pure (purity greater than 99.999 vol. %) hydrogen is produced.

Hydrogen saturation rate for electrolytic hydrogen and for molecular state was measured at near room temperature and 1—2 at pressure. It was shown that the hydrogen saturation rate un-

der electrolysis process ( $\approx 80 \text{ Ncm}^3 \text{ H}_2 / (\text{g} \cdot \text{h})$ ), is more than two orders of magnitude higher than in molecular driven regime ( $\approx 0.53 \text{ Ncm}^3 \text{ H}_2 / (\text{g} \cdot \text{h})$ ). The total volumetric quantity of hydrogen, saturated by the Pd-cathode, has been measured as  $\approx 840 \text{ Ncm}^3$  per hour. According to estimates, this corresponds to about 40% of the total production of electrolytic hydrogen.

The outgassing rate of hydrogen from palladium cathodes after exposure to ion current, during electrolysis process in the  $\text{H}_2\text{O} + 1 \text{ wt. \% NaHCO}_3$  electrolyte, has been measured in dependence on temperature and the time of exposure. The activation energy of the hydrogen outgassing from the Pd-cathode after one-hour exposure to an electrolytic current  $\approx 8 \text{ A}$  was found to be  $\approx 23$  or  $12 \text{ kJ/mol}$ , depending on the temperature range (20—100 and 300—650 °C, accordingly). An average value of activation energy across whole temperature range is  $E \approx 22.4 \text{ kJ/mol}$ .

The physical mechanism of possible influence of  $\beta \leftrightarrow \alpha$  transition in Pd on hydrogen outgassing has been suggested and discussed. In our case, hydrogen outgassing from  $\text{PdH}_x$  system is a fully-fledged multistage process with ever-changing activation energy on time. Nevertheless, to draw a well-founded conclusion, further studies are needed involving repeated hydrogen saturation of Pd-cathodes and thermal multi-cycling exposure. It would also be very important also to further analyze in details the impact of morphology and structural changes in Pd-cathodes after long time interaction with electrolytic hydrogen on their absorption and outgassing characteristics.

#### REFERENCES

1. Alefeld, G. & Völkl, J. (Eds.). (1978). *Hydrogen in Metals*. Vol. 1, 2. Berlin, Heidelberg, New York: Springer.
2. Glazunov, G. P., Bondarenko, M. M. & Konotopskiy, O. L. (2025). Hydrogen release from Pd electrodes after ion current impact during electrolysis process. *Problems of Atomic Science and Technology. Series: Plasma Physics*, No. 1(155), pp. 89-92. <https://doi.org/10.46813/2025-155-089>
3. Glazunov, G. P., Konotopskiy, O. L., Garkusha, I. E. & Elisieiev, D. V. (2024). Mass-spectrometric studies of hydrogen generation under electrolysis process with the using tube catalytic electrodes. *Problems of Atomic Science and Technology. Series: Physics of radiation damage and radiation materials science*, No. 4(152), pp. 148-151. <https://doi.org/10.46813/2024-152-148>
4. Glazunov, G. P., Bondarenko, M. M. & Konotopskiy, O. L. (2025). On the possible method of ultra-pure hydrogen generating. *Problems of Atomic Science and Technology. Series: Physics of Radiation Effect and Radiation Materials Science*, No. 5(159), pp. 140-145. <https://doi.org/10.46813/2025-159-140>
5. Adams, B. D. & Chen, A. (2011). The role of palladium in a hydrogen economy. *Materials today*, 14, No. 6, pp. 282-289. [https://doi.org/10.1016/S1369-7021\(11\)70143-2](https://doi.org/10.1016/S1369-7021(11)70143-2)
6. Glazunov, H. P., Andreiev, A. A., Baron, D. I., Volkov, Ye. D., Kytaievskiy, K. M., Konotopskiy, A. L., Lapshyn, V. I., Neklyudov, I. M. & Patokin, A. P. (2004). Hydrogen permeability and erosion of W-Pd bimetal system. *Fizyko-khimichna mekhanika materialiv*, No. 6, pp. 19-27 (in Ukrainian).
7. Glazunov, G. P., Andreev, A. A., Baron, D. I., Causey, R. A., Hassanein, A., Kitayevskiy, K. M., Konotopskiy, A. L., Lapshin, V. I., Neklyudov, I. M., Patokin, A. P., Surkov, A. E. & Volkov, E. D. (2006). Hydrogen permeability and erosion behavior of the W-Pd bimetallic systems. *Fusion Eng. Des.*, 81, Iss. 1-7, pp. 375-380. <https://doi.org/10.1016/j.fusengdes.2005.08.034>
8. Glazunov, G. P., Andreev, A. A., Baron, D. I., Volkov, E. D., Hassanein, A., Kitayevskiy, K. M., Konotopskiy, A. L., Lapshin, V. I., Neklyudov, I. M. & Patokin, A. P. (2005). Hydrogen saturation influence on erosion behavior of thin W-films under steady state nitrogen plasma impact. *Problems of Atomic Science and Technology. Series: Plasma Physics*, No. 2(11), pp. 107-109.
9. Glazunov, G. P., Andreev, A. A., Baron, D. I., Volkov, E. D., Causey, R. A., Hassanein, A., Kitayevskiy, K. M., Konotopskiy, A. L., Lapshin, V. I., Neklyudov, I. M. & Patokin, A. P. (2005). Kinetics of hydrogen permeation through W-Pd bimetallic systems. *Problems of Atomic Science and Technology. Series: Plasma Physics*, No. 2(11), pp. 82-84.

10. Federici, G., Skinner, C. H., Brooks, J. N., Coad, J. P., Grisolia, C., Haasz, A., Hassanein, A., Philipps, V., Pitcher, C. S. & Roth., J. (2001). Plasma-material interactions in current tokamaks and their implications for next step fusion reactors. *Nuclear Fusion*, 41, No. 12, pp. 1967-2137. <https://doi.org/10.1088/0029-5515/41/12/218>
11. Somenkov, V. A. & Shylshtein, S. Sh. (1978). Phase transitions of hydrogen in metals. Moscow: IAE (in Russian).
12. Glazunov, G. P. & Yuferov, V. B. (1980). On the use of palladium membranes in the thermonuclear devices. *Problems of Atomic Science and Technology. Series: Common and Nuclear Physics*, No. 4(14), pp. 91-95 (in Russian).
13. Glazunov, G. P., Volkov, E. D. & Hassanein, A. (2002). Bimetallic diffusion membranes: Possible use for active hydrogen recycling control. In: Hassanein, A. (Ed.). *Hydrogen and helium recycling at plasma facing materials*. NATO Science Series II, vol. 54 (pp. 163-176). Dordrecht: Springer. [https://doi.org/10.1007/978-94-010-0444-2\\_17](https://doi.org/10.1007/978-94-010-0444-2_17)
14. Grdeń, M., Czerwiński, A., Golimowski, J., Bulska, E., Krasnodębska-Ostręga, B., Marassi, R. & Zamponi, S. (1999). Hydrogen electrosorption in Ni—Pd alloys. *J. Electroanal. Chem.*, 460, Iss. 1-2, pp. 30-37. [https://doi.org/10.1016/S0022-0728\(98\)00330-1](https://doi.org/10.1016/S0022-0728(98)00330-1)

Received 19.02.2026

Г.П. Глазунов, <https://orcid.org/0000-0002-8895-927X>

М.М. Бондаренко, <https://orcid.org/0000-0001-5783-9788>

О.Л. Конотопський, <https://orcid.org/0000-0002-1622-6376>

Національний науковий центр “Харківський фізико-технічний інститут” НАН України,

Інститут фізики плазми, Харків, Україна,

E-mail: glazunov@ipp.kharkov.ua

#### КІНЕТИКА ДЕГАЗАЦІЇ І ПОГЛИНАННЯ ВОДНЮ ПАЛАДІЄМ У МОЛЕКУЛЯРНОМУ ТА ЕЛЕКТРОЛІЗНОМУ РЕЖИМАХ

Експериментально досліджено кінетику насичення та виділення водню з паладію в умовах взаємодії з молекулярним та електролітичним воднем за температури, близької до кімнатної, і тиску 1—2 атм. Ваговим методом визначено, що швидкість насичення воднем у процесі електролізу більш ніж на два порядки була вища, ніж за умов молекулярного режиму. За допомогою маспектрометричного методу встановлено, що після поглинання водню Pd-катодом під час електролізу та подальшого нагрівання його у високому вакуумі утворюється надчистий (понад 99,999 об. %) водень. За результатами вимірювання температурної залежності виділення водню було розраховано енергію активації цього процесу для Pd-катада після годинної дії іонного струму електролізу  $\approx 8 \text{ A} - E \approx 23 \text{ кДж/моль}$  або  $\approx 12 \text{ кДж/моль}$ , залежно від діапазону температур (20—100 або 300—650 °C). Середнє значення енергії активації для всього температурного діапазону вимірювань становило  $\approx 22,4 \text{ кДж/моль}$ . Отже, показано, що виділення водню із системи PdH<sub>x</sub> може бути багатостадійним процесом з постійно змінюваною енергією активації з часом. Для пояснення такої поведінки водню під час процесу газовиділення також розглянуто і проаналізовано фізико-хімічні механізми та вплив переходу  $\beta \leftrightarrow \alpha$  у системі PdH<sub>x</sub>.

**Ключові слова:** водень, паладій, електроліз, енергія активації, абсорбція, газовиділення.